The effect of initial temperature and oxygen ratio on air-methane catalytic combustion in a helical microchannel using molecular dynamics approach

Qing An [a], Ali Basem [b], As'ad Alizadeh [c], Ameer H. Al-Rubaye [d], Dheyaa J. Jasim [e], Miao Tang [a], Soheil Salahshour [f, g, h], Rozbeh Sabetvand [i, *]

[a] School of Artificial Intelligence, Wuchang University of Technology, Wuhan, 430223, Hubei Province, China
[b] Faculty of Engineering, Warith Al-Anbiyaa University, Karbala, 56001, Iraq
[c] Department of Civil Engineering, College of Engineering, Cihan University-Erbil, Erbil, Iraq
[d] Department of Petroleum Engineering, Al-Kitab University, Altun Kupri, Iraq
[e] Department of Petroleum Engineering, Al-Amarah University College, Maysan, Iraq
[f] Faculty of Engineering and Natural Sciences, Istanbul Okan University, Istanbul, Turkey
[g] Faculty of Engineering and Natural Sciences, Bahcesehir University, Istanbul, Turkey
[h] Department of Computer Science and Mathematics, Lebanese American University, Beirut, Lebanon
[i] Department of Energy Engineering and Physics, Faculty of Condensed Matter Physics, Amirkabir University of Technology, Tehran, Iran

GRAPHICAL ABSTRACT
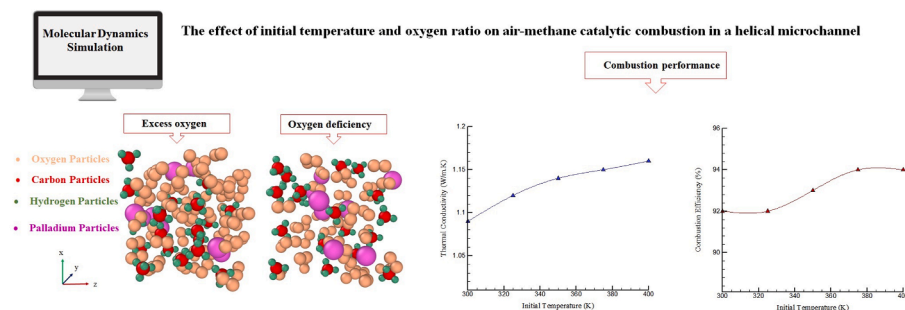
ARTICLE INFO

ABSTRACT

In industrial environments where combustion (Com.) is widely carried out, such as steam power plants, gas turbines, etc., the most common way to express the amount of oxygen consumption is its excess percentage in addition to the stoichiometric ratio, and the nearness of a catalyst causes combustion to happen at a high ratio. There are different influential factors in catalytic combustion, such as initial temperature (IT). The current study uses the molecular dynamics (MD)

* Corresponding author.
  E-mail address: rozbeh.sabetvand@iaukhsh.ac.ir (R. Sabetvand).

Atomic behavior

method to examine how the IT and oxygen ratio affect air-methane catalytic combustion in a helical microchannel. The LAMMPS package was used to conduct this investigation. This study examines how simulated structures function during burning in excess oxygen (EO) and oxygen deficiency (OD). Furthermore, palladium was used as a catalyst with an atomic ratio of 4 %. The findings show that raising the IT may enhance its atomic behavior (AB) and thermal performance (TP). The maximum velocity (MV) and maximum temperature (MT) increased from 0.26 Å/ps and 1617 K to 0.45 Å/ps and 1891 K in EO as IT increased from 300 to 700 K. By accelerating the particle velocity, it is anticipated that the catalytic combustion process would proceed more quickly. As a result, after increasing the IT to 700 K, the heat flux (HF), thermal conductivity (TC), and combustion efficiency (CE) increase to 2101 W/m^2, 1.23 W/m. K, and 93 %, respectively. On the other hand, the results show that increasing IT affects combustion performance in the presence of OD. In the presence of OD, the MV and CE converge to 0.38 Å/ps and 94 % at 700 K. Therefore. It can be concluded that the atomic ratio of oxygen and the IT can significantly affect combustion process.

Abbreviations

Com.	Combustion
IT	Initial temperature
MD	Molecular Dynamics
EO	Excess oxygen
OD	Oxygen deficiency
AB	Atomic behavior
TP	Thermal performance
MV	Maximum velocity
MT	Maximum temperature
Den	Density
HF	Heat flux
TC	Thermal conductivity
CE	Combustion efficiency
RDF	Radial distribution function
EAM	Embedded-Atom Method
LJ	Lennard-Jones
LAMMPS	large-scale atomic/molecular massively parallel simulation

Nomenclature

r_{ij}	The distance between particles (m)
u_i	The potential of a particle (eV)
ε_{ij}	Depth of the potential well (kcal/mol)
σ_{ij}	Finite distance in which the potential is zero(Å)
r	The distance of the particles from each other
U_{ij}	The electric potential (eV)
V	The total volume of particles (Å^3)
k_B	Boltzmann constant (1.380649 × 10^{-23} J K^{-1})
T	The system temperature (K)
J	The heat flux(W/m^2)
m_i	The mass of the particle(g)
a_i	The acceleration of the particle (m·s^{-2})
N_{fs}	The number of degrees of freedom
F_α	Constant coefficient between 0 and 1
ρ_β	An attraction force caused by the presence of particles in the simulated box
φ_β	A repulsive force caused by atomic charge density

1. Introduction

Exothermic complex consecutive reactions between an oxidizing or oxidizing substance and Fuel, which are accompanied by heat, light, or both and appear in the form of a flame, are called combustion or burning [1]. combustion is divided into several categories based on velocity, incompleteness, or completeness: fast, slow, complete, and incomplete. Common fuels are usually made of organic compounds (especially hydrocarbons) in the gaseous, liquid, or solid form [2]. A substance reacts with an oxidizing agent such as oxy-

gen or fluorine in a complete combustion reaction. The reaction products will combine both, i.e., explosive and oxidizing agents. The most oxidizing substance used for burning is oxygen, which is abundant in the air around us [3,4]. When oxygen from the air reacts, some dangerous nitrogen compounds (NO_x) are also formed due to the heat from burning and combining with oxygen. However, a significant reduction in NOx emissions was achieved by adopting a premixed operation mode in which the flame temperature is reduced, and the NO_x level is greatly reduced [5]. In industrial environments where combustion is widely carried out, such as steam power plants, gas turbines, etc., the most common way to express the amount of oxygen consumption is its excess percentage in addition to the stoichiometric ratio [6]. From a practical point of view, although combustion is one of the main sources of air pollution, in the process of air pollution control, its purpose is to convert air pollutants into harmless carbon dioxide or water. Therefore, the combustion device is designed to control the release of air pollutants in order to make the oxidation reactions as complete as possible and leave the minimum unburned compounds [7]. To achieve proper efficiency in combustion, the four main factors of oxygen, temperature, agitation, and time are essential. During combustion, the amount of accessible oxygen determines the final products obtained. In low oxidation, soot and carbon monoxide are the by-products of combustion, while with sufficient oxygen, carbon monoxide will be the by-product of combustion. Although combustion starts as soon as a substance reaches the point of burning, to control air pollution, it is necessary to maintain the temperature at the ashing point (where the heat generated by the reaction is greater than the heat lost in the surrounding environment) [8]. Understanding and mastering combustion processes is crucial due to the major concerns about environmental pollution caused by Com.. We can build engines that are more efficient and reduce the amount of pollution produced by doing so by gaining a basic understanding of how combustion works.

Due to the high importance of combustion in various industries, many researchers have studied the combustion process and its effective parameters. Mousavi et al. [9] investigated the effects of adding NH_3 to the H_2/CH_4 reactive mixture under a mild combustion regime. The results show that contrary to what was reported for conventional combustion, the addition of NH_3 under mild conditions did increase NO emissions, while the NO_2 mass fraction slightly decreased. Ariemma et al. [10] studied the stability and emission of NO_x in ammonia/methane Com.. They revealed that the interplay of the main chemical pathways of methane and ammonia affects the DeNO$_x$ channel by the observed increase in NO_x emissions. Choi et al. [11] investigated combustion of a drop of carbon black nanofuel/dilute ethanol under high-pressure conditions. They demonstrated that although the burning rate increased due to heat radiation, increasing the carbon black content did not substantially alter the ignition delay. Nam et al. [12] studied the high-pressure combustion characteristics of a single butanol gel fuel drop. The findings demonstrate that, in contrast to pure liquid Fuel, the behavior of combustion is insensitive to pressure owing to the effect of the gel layer on the droplet surface. Liu et al. [13] thoroughly examined the Al/AP combustion process, and the findings served as a theoretical basis for elucidating the combustion process and enhancing the energy release properties of solid fuels incorporating aluminum-based AP. Gas-phase combustion can only take place within a certain range of flammability, and the temperatures generated during combustion may exceed 1600 C. Low temperature, flameless Com. is known as catalytic combustion. This results in less nitrogen oxide being released. Extensive research has been done on the use of catalysts in combustion process. For example, Chen et al. [14] used calcined nickel hydroxide in the catalytic combustion process. The findings demonstrated that the catalyst's structure is stable when the temperature increases from 400 K to 500 K. Shao et al. [15] studied the usage of CuO and $CuCo_2O_4$ in the methane combustion catalytic process. The results indicate that applying these two catalysts improved combustion process. Particularly, combustion takes place in extreme physical conditions, including high pressures and temperatures that may reach several thousand degrees. In addition, numerous elementary processes in combustion often occur on timescales of less than 1 ps. Due to these severe physical conditions, real-time experimental studies of combustion are highly challenging, if not impossible. Therefore, individual reactions rather than the intricate reaction pathways involved in combustion are the focus of the majority of experimental studies of chemical reaction mechanisms. Experimental procedures often take more time and money than simulation approaches [16]. The MD approach allows for atomic-level control of the environment. Also, creating and checking super-crisis conditions can also be checked with this method. Reactive MD simulation may build the full interconnected network of reactions in a Com. system, as opposed to more conventional theoretical techniques like transition sate theory and quantum collision theory, which concentrate on investigating a particular process.

Liu et al. [17] studied the effect of an initial pressure and palladium catalyst on the catalytic combustion of CH_4 and air. They demonstrated that the addition of a Pd catalyst significantly enhanced the TP of the simulated structure. The maximum Den. did not significantly change when the pressure was increased, but the values for MV and MT changed regarding the restriction on atomic oscillations. Feng et al. [18] studied the methane combustion in the existence of Pt/Graphene catalyst utilizing MD simulation. The findings demonstrated that the Pt@FGS reaction drastically lowers the activation energy compared to pure methane combustion, improving catalytic activity. Wang et al. [19] simulated the reaction mechanism for NH_3/CH_4 Com.. The findings demonstrate that high pressure complicates NH_3/CH_4 combustion process pathways by enhancing molecular/atomic collisions. Liu et al. [20] investigated the mechanisms of CH_4/H_2 blended combustion by MD simulation. The findings indicated that as the temperature rises, the encouraging effect of CH_4 combustion lessens as hydrogen concentration increases. Habibollahi et al. [21] simulated Com. behavior of coated Al hydride nanoparticles. The findings demonstrated that by increasing the atomic percentage of ethanol coating, HF increases from 3.88 to 7.01 W/m^2, respectively.

Previous studies have shown that MD can accurately calculate the combustion behavior of different structures [22–24]. In previous research, combustion process and its characteristics affected different factors such as adding nanoparticles, catalysts, IT, and so on were studied by many researchers. They demonstrated that better combustion and improved thermal behavior result from increasing temperature and adding a catalyst.

According to earlier research, the catalytic combustion of air-methane had not been examined in relation to the atomic percentage of oxygen and IT. This study used the MD method to examine how the IT and oxygen ratio affected the AB and TP of simulated struc-

tures under EO and OD during air-methane catalytic combustion in helical microchannels. The AB and TB are investigated at different temperatures of 300, 400, 500, 600, and 700 K, and by checking the maximum Den., MV, MT, TC, HF and CE.

2. Numerical method

2.1. MD simulation details

The MD method was utilized in this work to examine how IT affected the combustion process when various oxygen atom ratios were present. Calculations were represented using the LAMMPS software [25,26]. The samples are in their most ideal condition when there is a stoichiometric amount of oxygen within the simulation box. The samples were modeled in a Fe/Cu-microchannel by Avogadro software as a $1 \times 1 \times 1 \ \mu m^3$ simulation box with a periodic boundary condition in all directions. The initial pressure and temperature, set to 0 bar and 300 K, respectively, were controlled by the NPT ensemble and Nose-Hoover thermostat. By choosing constant boundary constraints, it is possible to limit the size of atomic structures in three directions, and using periodic boundary requirements, it is possible to repeat certain directions. The boundary conditions are fixed. The initial and ultimate pressure and temperature parameters must be established before the combustion process in this sample can be put into action by raising the simulation box's temperature. The temperature and pressure of the simulated structures will thus be adjusted using the Nose-Hoover thermostat and the NPT ensemble. The structure will equilibrate at 300K during the first simulation period. After the simulated sample has been tested for atomic stability and thermodynamic equilibration and switched to the NVE ensemble, the temperature of the sample will be increased until combustion occurs. A general flowchart of MD simulation and A schematic of the simulated structure under various oxygen ratios (EO and OD) were shown in Fig. 1. Also, please see appendix A for more details about MD method.

3. Results and discussion

3.1. Validation

In this part, the RDF of O_2 was calculated to validate the results of MD simulations. Physically, the RDF in an atomic structure represents particles' relative arrangement. Calculating the RDF was a compelling way to recognize between different atomic structures, agreeing with the basic concepts of the MD simulation. The atomic neighbors of the core atom are represented by the peaks formed in the RDF of an atomic sample from a physical perspective. As a result, this function had a distinct peak for various gas-phase structures, after which its numerical value tended to be constant. On the other hand, the RDF for atomic structures in the liquid phase showed a clear peak and multiple subsidiary peaks. Similar peaks of approximately equal size were expected for the radial distribution function of solid structures. Fig. 2 shows the radial distribution function of oxygen molecules defined after 10 ns and after observing the thermodynamic equilibrium in atomic structure. The pattern of this radial distribution function was not changed over time in atomic samples, and consequently, it could be compared with previous results. Comparing this quantity showed an acceptable correspondence between the simulations performed and previous studies [28,29], which showed the scientific validity of the results obtained from MD simulations. Based on the diagram, the initial peak occurred after 10 ns near the 2.5 Å point.

3.2. Atomic behavior in the presence of EO

The combustion process was examined in artificial prototypes with too much oxygen following a sample equilibrium check. The catalytic combustion of CH_4 at a low temperature is becoming progressively key to controlling unburned CH_4 emanations from natural gas vehicles and control plants. The presence of catalysts empowers the complete oxidation of CH_4 at much lower temperatures (ordinarily 400 K) so that the arrangement of toxins can be generally avoided [30]. Much research has been done concerning the effect of the IT (the temperature of entering the materials into the Com. chamber) on combustion of methane at low temperatures [31]. For example, Gu et al. [32] studied the burning of methane in combustion chamber with an IT = 400 K. Yan et al. [33] also investigated the effect of IT on methane burning. Their results show that the conversion rate is high at 400 K and increases with increasing temperature.

Fig. 3 depicts changes in maximum Den. with increasing IT and an abundance of oxygen. As can be seen, the maximum Den. with an IT of 300 K was 0.131 atom/Å^3. With the increase in IT, it went through an upward trend. To be more precise, by increasing the IT from 300 K to 700 K, the density rose to 0.120 atom/Å^3. Den. is inversely proportional to the temperature. Heating a substance causes molecules to velocity up and spread slightly further apart, occupying a larger volume that decreases Den. [34]. The value of maximum Den. in the presence of EO is displayed in Table 1. The results are consistent with those of Liu et al. [35]. Their results show that the Den. decreases with increasing IT. The value of maximum Den. in the presence of EO is displayed in Table 1.

In Fig. 4, the MV changed by increasing IT and additional oxygen. The results demonstrate that a higher starting temperature caused a higher sample velocity. The range of atoms' oscillations is increased by raising the IT, which also raises atom movements and kinetic energy. As the kinetic energy raised, based on $\frac{1}{2}mv^2 = \frac{3}{2}KT$ the velocity of atoms increased [36]. Based on the diagram, by increasing the IT from 300 to 700 K, the MV converged from 0.26 Å/ps to 0.45 Å/ps. The different values of sample MV concerning IT changes are given in Table 1.

In the presence of EO, Fig. 5 shows the changes in MT with increasing IT. By raising the IT, temperature changes show an upward trend as density and velocity increase. In other words, from an IT of 700 K, the highest temperature rose to 481 K. After ensuring the atomic stability and thermodynamic equilibration of the simulated sample, changed to NVE ensemble the temperature of the sample will be increased and the combustion process occurs. Catalytic combustion is made possible at lower temperatures than would otherwise be feasible by the presence of a combustion catalyst. The findings demonstrate that when the IT increases, the head and movement of the atoms also increase, increasing the velocity of the molecules. The temperature rises in direct proportion to the velocity of

(a)

- Oxygen Particles
- Hydrogen Particles
- Palladium Particles
- Carbon Particles

x
y
z

(b)

(c)
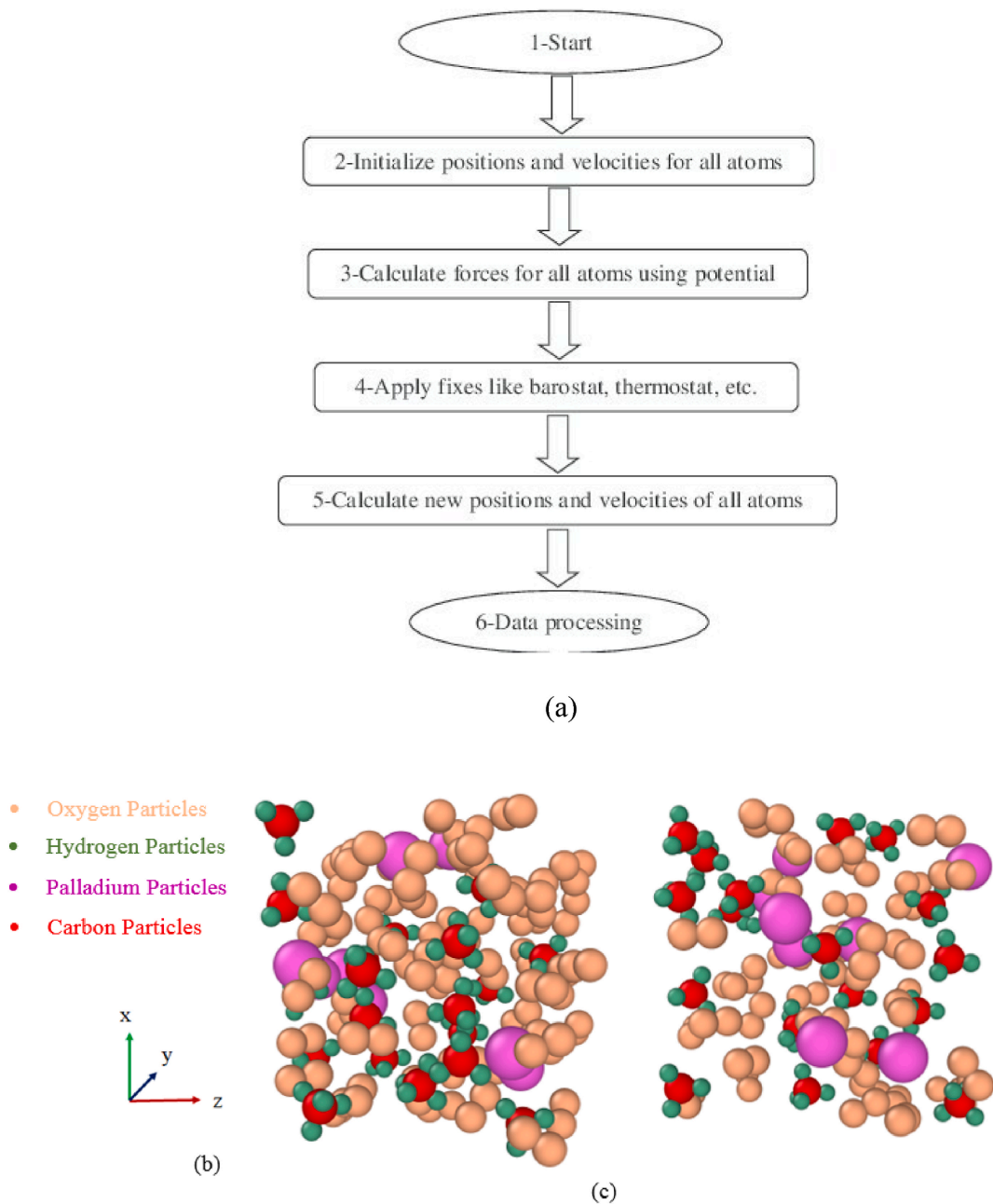
Fig. 1. a) The flowchart of the MD simulation [27]. A structure schematic with a) EO and b) OD.

the atoms, which in turn accelerates combustion process. Numerical values by increasing IT within the presence of EO are presented in Table 1.

3.3. Thermal performance within the presence of EO

The amount of HF, TC, and CE by increasing IT in EO was considered to indicate combustion performance. Fig. 6 displays the modifications in HF in a simulated atomic sample brought on by adding varying levels of IT when there was a lot of oxygen. Based on the results, the HF was 2046 W/m^2 with an IT of 300 K. However, by increasing the IT to 700 K, the HF value converges to 2101 W/m^2 as a maximum value. Heat transfer is directly proportional to the velocity of molecules and temperature. As the IT increases, the range of oscillations of atoms increases, and as a result, the velocity increases. Increasing the temperature and velocity makes heat transfer better and faster [37]. Precisely, within the presence of EO, the value of HF increased by increasing the IT.
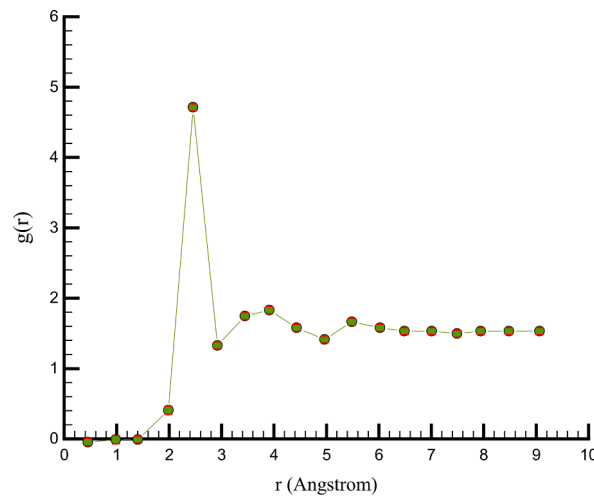
Fig. 2. The RDF of O_2 inside the simulation box after 10 ns.
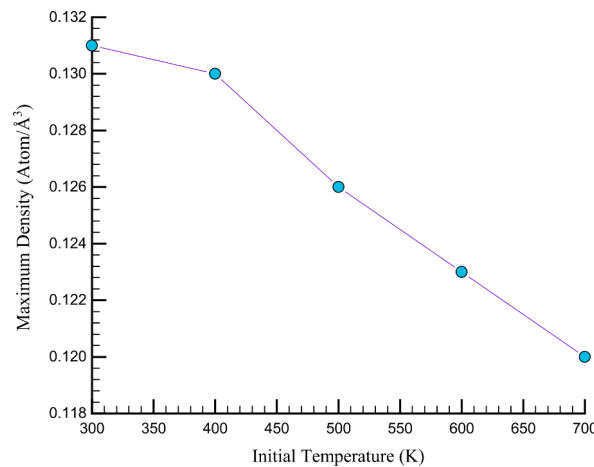
Fig. 3. The change in maximum Den. by increasing IT within the presence of EO.

Table 1
The change in maximum Den., MV, and MT with increasing IT within the presence of EO.

IT (K)	Maximum Den. (atom/Å³)	MV (Å/ps)	MT (K)
300	0.131	0.26	1617
400	0.130	0.32	1788
500	0.126	0.34	1805
600	0.123	0.39	1852
700	0.120	0.45	1891

Fig. 7 shows the changes in TC by increasing IT and an abundance of oxygen. As can be observed, the value of TC grew as the IT did as well. According to the diagram, the TC with the IT of 300 K was 1.16 W/m.K. After increasing the IT to 700 K, the maximum TC reached 1.23 W/m.K. Therefore, IT had a direct effect on simulated structures.

Additionally, Fig. 8 illustrates the information about CE changes by increasing IT in the presence of extra oxygen. The findings demonstrate that the value of CE increased to 93 % with an IT increase of 700 K. These findings show that raising the IT enhanced the structure's CE. The results are consistent with those of Geng et al. [38]. The changes in HF, TC, and CE with incrementing IT within the presence of EO are displayed in Table 2.

To ensure complete combustion of the fuel used, combustion chambers are supplied with excess air. Excess air increases the amount of oxygen to combustion and the combustion of fuel (Fig. 9). The CE increases with increased excess air - until the heat loss in the excess air is larger than the heat provided by more efficient Com. [39]. The chemical structure of the hydrogen molecule is the H–H band, which requires less energy for breakdown, and hydrogen induces catalytic surface chemical reaction under low reaction
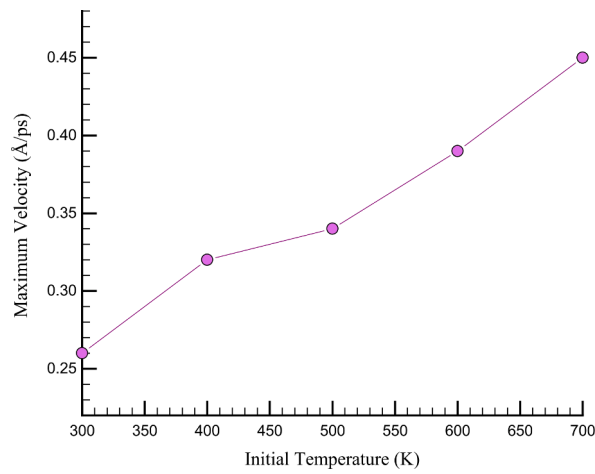
Fig. 4. Change in MV with increasing IT within the presence of EO.
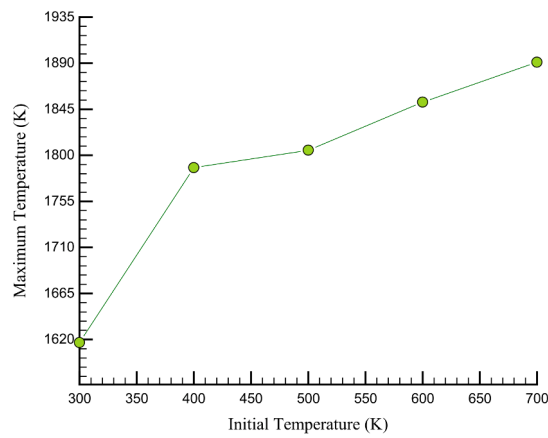
Fig. 5. The change in MT over the IT within the presence of EO.
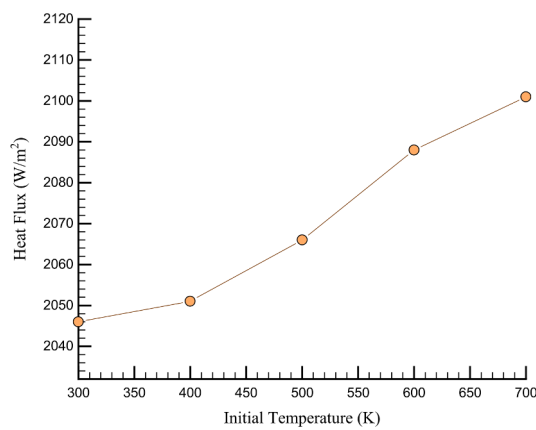
Fig. 6. The change in HF by increasing IT within the presence of EO.

temperatures. The CE is high and near 89 % when IT is specified with a fixed value of 400 K, and CE is near 93 %, along with IT increases to 700 K.

According to the diagram above, increasing oxygen diminishes efficiency. CE initially increments with increasing EO levels and then diminishes. This is due to increased CO and hydrocarbon emissions as the excess air level increases to higher levels [41].
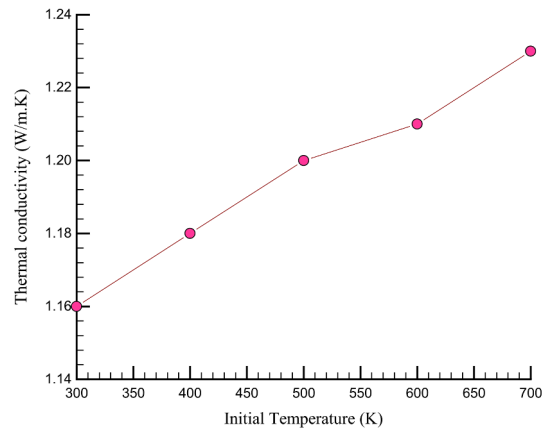
Fig. 7. The change in TC by increasing IT within the presence of EO.
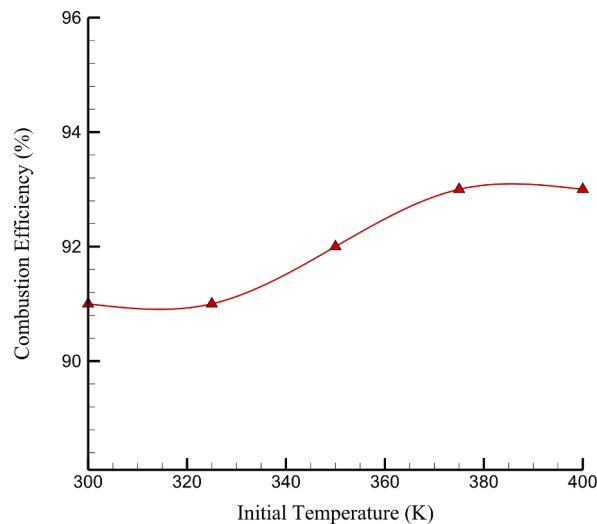
Fig. 8. The change in CE by increasing IT within the presence of EO.

Table 2
The change in TC, HF, and CE by increasing IT in the presence of EO.

IT (K)	HF (W/m^2)	TC (W/m.K)	CE (%)
300	2046	1.16	89
400	2051	1.18	90
500	2066	1.20	92
600	2088	1.21	92
700	2101	1.23	93

3.4. Atomic behavior in the presence of OD

This study section discovered how the simulated sample's AB changed when the IT increased and OD was present. Fig. 10 displays the changes in maximum Den. caused by rising IT and a lack of oxygen. The volume is directly proportional to the IT, whereas the Den. of the substance is inversely proportional to the volume, and thus, it is inversely proportional to the IT. If we raise the IT, the Den. of the substance decreases and vice-versa. As observed, when an IT of 700 K was applied, the maximum Den. converged to 0.087 atom/Å^3. It is concluded that there was an upward trend in the density of simulated samples related to increasing IT. According to the findings, raising the IT when there was an excess of oxygen had a greater effect on increasing the sample density than when there was an OD.

Additionally, the changes in MV caused by raising the IT when there was an OD were examined in Fig. 11. By raising the IT, the sample's MV increased as a Den.. From a numerical perspective, by raising the IT from 300 K to 700 K, the simulated sample's MV increased from 0.28 Å/ps to 0.38 Å/ps.
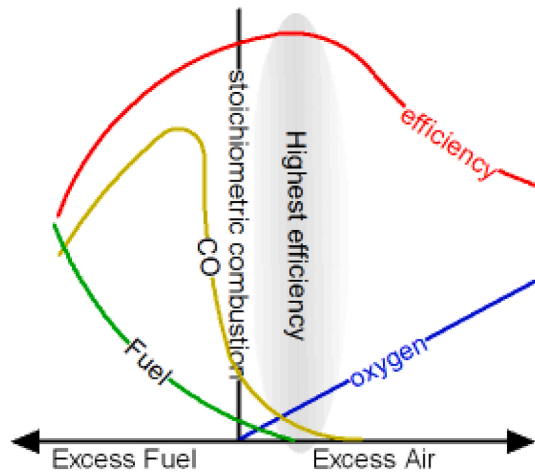
Fig. 9. CE diagram in terms of excess air [40].
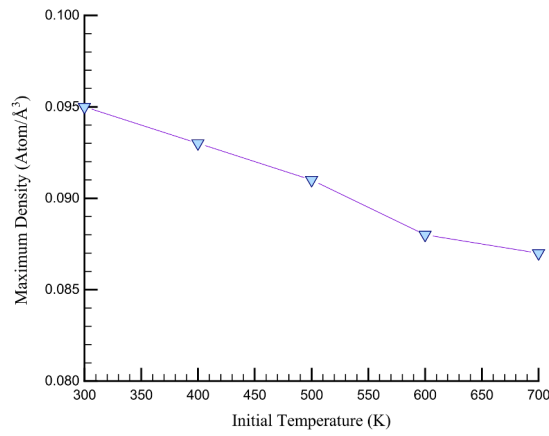
Fig. 10. The maximum Den. changes by increasing IT in the presence of OD.
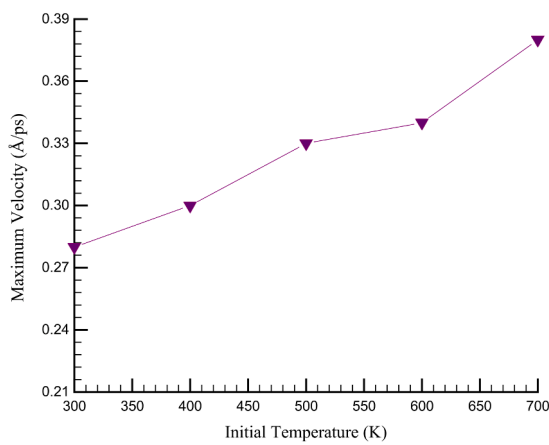
Fig. 11. The change in MV over IT in the presence of OD.
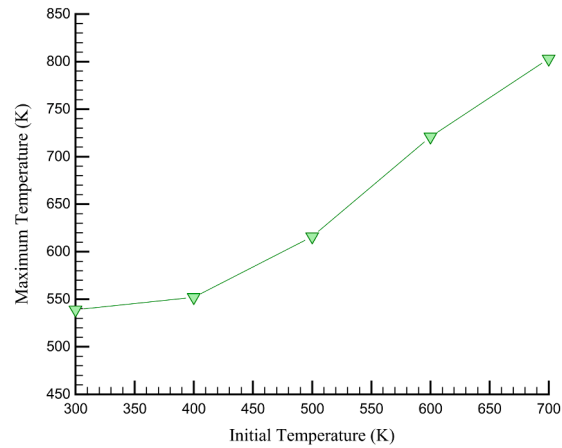
Fig. 12. The change in MT over IT within the presence of OD.

Table 3
The change in maximum Den., MV, and MT with increasing IT in the presence of OD.

IT (K)	Maximum Den. (atom/Å^3)	MV (Å/ps)	MT (K)
300	0.095	0.28	539
400	0.093	0.30	552
500	0.091	0.33	616
600	0.088	0.34	721
700	0.087	0.38	803
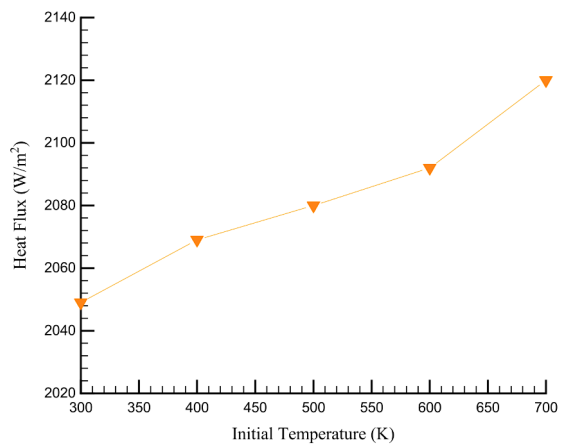
Fig. 13. The change in HF by increasing IT within the presence of OD.

In Fig. 12, it was examined how the MT changed as the IT increased when there was an oxygen deficiency. As a consequence, the temperature value increased and converged from 539 K to 803 K when the IT rose from 300 K to 700 K. Table 3 lists the numerical values of maximum Den., MV, and MT. The IT had a higher effect on raising the sample IT when there was an OD.

3.5. Thermal performance in the presence of OD

HF, TC, and CE parameters were then examined with an increase in IT while an OD was present to assess thecombustion performance. The IT changes in HF in the presence of OD are shown in Fig. 13. An increase in IT caused an increase in HF. Numerically, by increasing the IT from 300 to 700 K in the simulated sample, HF converges from 2049 to 2120 W/m². Increasing HF can be a sign of optimal TP.

Fig. 14 depicts the change in TC by rising IT when there is a lack of oxygen. The findings show that by raising the IT from 300 to 700 K, the HF of the simulated sample increased from 1.23 to 1.29 W/m. K. As a result, OD caused the sample's HF to increase more than the oxygen surplus did.
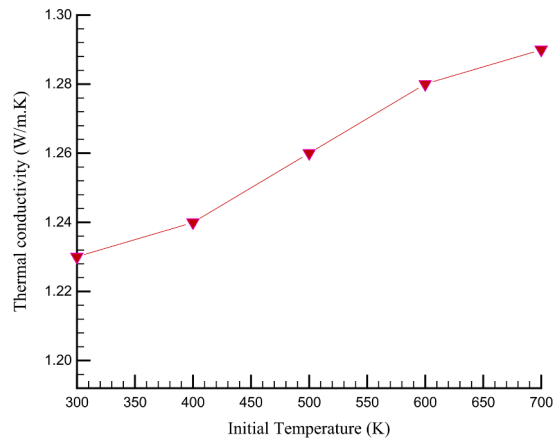
Fig. 14. The change in TC by increasing IT within OD's presence.

Fig. 15 depicts the changes in CE caused by an increase in IT and OD. With an IT change of 700 K, the value of CE converges to 94 %. The CE of the simulated sample varied as a consequence, depending on whether there was an EO or OD. In general, the IT had a greater effect on TP in OD than in the presence of adequate oxygen, maximizing the thermal behavior. Generally, the IT in the presence of OD is more effective on the TP of the sample than in the presence of EO, optimizing the sample's thermal behavior. Incomplete air causes incomplete combustion, and as a result, less carbon dioxide is produced and reduces CE. Table 4 lists the numerical values of HF, TC, and CE changes.

4. Conclusion

The effect of IT with various values of 300, 400, 500, 600, and 700 K on air-methane catalytic combustion in the presence of various oxygen atom ratios was explored in the current research. LAMMPS software was used to complete this investigation in 20 ns under the direction of MD. The structure's atomic and Com. performance was then examined in response to changes in maximum Den., MV, MT, HF, TC, and CE. The main outputs of current research can be categorized as follows:
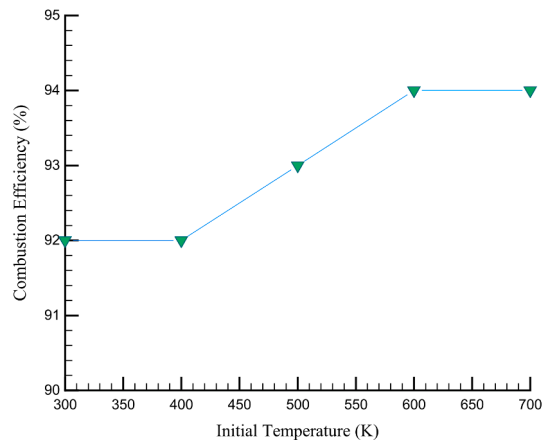
Fig. 15. The change in CE by increasing IT in the presence of OD.

Table 4
The change in HF, TC, and CE by increasing IT in the presence of OD.

IT (K)	HF (W/m^2)	TC (W/m.K)	CE (%)
300	2049	1.23	92
400	2069	1.24	92
500	2080	1.26	93
600	2092	1.28	94
700	2120	1.29	94

- In the presence of EO, the Den., MV, and MT increase as the IT increases. By increasing the IT from 300 K to 700 K, the Den. decreased and reached the maximum value of 0.120 atom/Å^3. Moreover, the MV of the sample increases from 0.26 A/ps to 0.45 A/ps. Moreover, the MT converges to 1891 K by increasing the IT.
- In the presence of EO, combustion performance of the simulated sample improves by increasing the IT. In other words, HF, TC, and CE increase by rising IT.
- In the presence of EO, by increasing the IT from 300 K to 700 K, the HF converges from 2046 to 2101 W/m^2, and the TC reaches from 1.16 to 1.23 W/m.K, and CE increases from 89 % to 93 %.
- In the presence of OD, increasing IT caused an increase in atomic behavior parameters, such as Den., MV, and MT. To be more precise, by increasing the IT from 300 to 700 K, the Den. of the sample converged from 0.095 to 0.087 atom/Å^3, the MV of the simulated sample increased from 0.28 to 0.38 A/ps, and the MT reached 803 K.
- In the presence of OD, the combustion performance of the sample was optimized by increasing IT from 300 to 700 K. Precisely, HF, TC, and CE reached 2120 W/m^2, 1.29 W/m.K, and 94 %,
- Comparatively, the IT increase in the presence of OD in the simulated sample was more than in EO.

Future work

The aim of this article was the effect of IT (inlet temperature) and oxygen content in the catalytic combustion process in the helical microchannel. In future works, the authors will investigate the effect of the type and shape of the microchannel on combustion process.

CRediT authorship contribution statement

Qing An: Investigation, Writing – original draft. **Ali Basem:** Investigation, Writing – original draft. **As'ad Alizadeh:** Formal analysis, Writing – original draft. **Ameer H. Al-Rubaye:** Supervision, Writing – review & editing. **Dheyaa J. Jasim:** Methodology, Project administration. **Miao Tang:** Validation, Methodology. **Soheil Salahshour:** Formal analysis, Writing – review & editing. **Rozbeh Sabetvand:** Conceptualization, Data curation, Formal analysis.

Declaration of competing interest

The authors declare that they have no known competing financial interests or personal relationships that could have appeared to influence the work reported in this paper.

Data availability

No data was used for the research described in the article.

Appendix A

A-1. MD method

MD simulation approach uses the thermodynamic, equilibrium, and transfer properties of materials in diverse phases (solid, liquid, and gas) using physical attributes such as force, velocity, and particle position. The MD simulation approach calculated the motion of particles shown in a model system as they interacted and exerted forces on one another over an extended period of time.

The MD simulation method is a specific method based on Newton's second law. By integrating Newton's second law, the path of particle movement (including location, velocity and particle) is obtained, and by averaging the obtained values, the macroscopic properties of the system can be obtained. The reason why this method is specific is that by determining the location and velocity of each particle in the current time, the state of a particle-based system in the past and future can be predicted at each time step, and communication can be established between them. In a general summary, it can be said that the MD simulation method is a standard method that allows the calculation of forces and energies between particles at any given temperature [25].

The MD simulation method is a reliable and reliable method for studying at micro and nano scales. The process of phase change and their effects on heat transfer should be used in detail. In fact, all these methods are a bridge between quantum mechanics and macro (continuous) scale mechanics, which are used to model particle-based systems depending on the length and time scales of the problem [26]. As a result, in this research, the catalytic combustion of methane/air was investigated by means of MD simulation. Using simulation results, it is possible to predict the behavior of other gases and use its results in various industries such as aerospace, petrochemical, steel industries, etc.

This method obtains the movement path of the particles by solving Newton's equations of motion, and this is done with an external force (F_i) which is obtained from the potential function (U) and enters the particle i [27]:

$$F_i = m_i a_i = -\nabla_i U = -\frac{dU}{dr_i} \tag{a-1}$$

After setting the initial circumstances, the intermolecular and intramolecular forces are calculated and integrated using the equations of motion. The velocity-Verlet algorithm is one of the most common and fast algorithms [28,29].

The equilibrium method applying Green-Kubo function (Eqs. a-2 and a-3) was used to study the TC of simulated system [30]:

$$K = \frac{V}{k_B T^2} \int_0^\infty \left(J_x(0) J_x(t) \right) dt = \frac{V}{3 k_B T^2} \int_0^\infty \left(J(0). J(t) \right) dt \tag{a-2}$$

where V is the volume that the simulation's current particles have taken up, KB denotes Boltzmann's constant, T denotes the temperature, and J denotes HF. The mean of the HF matching function is referred to by the term within the integral, on the other hand. The HF vector is obtained from the equation shown below [30]:

$$\begin{aligned}
J &= \frac{1}{V} \left[\sum_i E_i v_i - \sum_i S_i v_i \right] \\
&= \frac{1}{V} \left[\sum_i E_i v_i - \sum_{i<j} \left(f_{ij} v_j \right) x_{ij} \right] \\
&= \frac{1}{V} \left[\sum_i E_i v_i - \frac{1}{2} \sum_{i<j} \left(f_{ij}. \left(v_i + v_j \right) x_{ij} \right) \right]
\end{aligned} \tag{a-3}$$

In Eq. (3), j and i are two carbon atoms at the two ends of bond, and E_i is the total energy for each of the particles in the system, v_i is the velocity of particles, S_i is the entropy of system, f_{ij} is the force, and V is the total volume. The specification of the potential function and interparticle forces is a crucial element that must be considered in the MD simulations. Definitions of potential functions or descriptions of words pertaining to the interactions of system components are necessary for the MD simulation. The interactions are often split into two categories: bonded interactions and non-bonded interactions [25,31,32]. The interaction potential of particles is studied by means of the Lennard-Jones (LJ), Embedded Atom Model (EAM), and Coulomb potential functions. The common model of atomic bonding in metal systems, which is expressed as follows, is shown by the potential function of EAM [25]:

$$U_i = \sum_{i=1}^{N-1} \sum_{j=i+1}^{N} \varphi \left(r_{ij} \right) + \sum_{i=1}^{N} F \left(\rho_i \right) \tag{a-4}$$

where the interatomic energy and potential embedding function are denoted by $\Phi(r_{ij})$ and $F(\rho_i)$, respectively. A simple mathematical model called the LJ potential function is used to approximation the interactions among neutral particles [31]:

$$U_{LJ} = 4 \varepsilon_{ij} \left[\left(\frac{\sigma_{ij}}{r_{ij}} \right)^{12} - \left(\frac{\sigma_{ij}}{r_{ij}} \right)^6 \right] r < r_c \tag{a-5}$$

where, ε_{ij} is the depth of potential well, σ_{ij} is the finite distance in which the potential is zero, and r_c shows cut-off radii. The numerical values of ε_{ij}, σ_{ij}, and r_c for all particles are reported in Table a- 1.

Table a-1
LJ potential parameters [33,34].

Atom	ε (kcal/mol)	σ (Å)	Cut-off radii (Å)
H	0.044	2.886	12
O	0.06	3.500	12
C	0.105	3.851	12
Pd	0.048	2.899	12

The ε_{ij} and σ_{ij} of each particle are obtained as follows [33]:

$$\varepsilon_{ij} = \sqrt{\varepsilon_i \varepsilon_j} \tag{a-6}$$

$$\sigma_{ij} = \frac{\sigma_i + \sigma_j}{2} \tag{a-7}$$

The following diagram illustrates how Coulomb's potential function is used to calculate the static electric charge forces that absorb or repel particles [32]:

$$U_{ij}(r) = \frac{-1}{4 \pi \varepsilon_0} \frac{q_i q_j}{r_{ij}^2} \tag{a-8}$$

A-2. Stability Process

By analyzing kinetic and total energy changes by the NPT ensemble, the simulated sample at 300 K and 0 bar arrived to equilibrium. A reversible process is said to be in dynamic equilibrium when the forward and reverse processes occur at the same rate, result-

ing in no observable change in the system. Convergence in MD simulation has a well-known definition: we discovered a set of atomic coordinates matching to a local Energy minimum as a function of the selected force field [39,42,43]. The convergence idea in MD simulation was based on "Ergodic Hypothesis: The long time average was equal to the ensemble average in the limit of an infinite number of members in the ensemble" [40]. As noted above, it depended on what quantity we were looking at. Convergence of Energy (potential, kinetic, total), temperature, etc. Fig. A-1 shows the changes in the simulated sample's kinetic and total energy during the course of the experiment. The kinetic energy value quantitatively converged to 223.07 V after 10 ns. This finding supports the notion that atomic sample kinetic energies converged. The atomic samples' equilibrium will be shown by this convergence to a certain value brought about by a reduction in this amount's change range. The total energy also converged at −610.5 eV. The fact that this quantity is negative shows that interatomic attraction forces are more powerful than the mobility of the atomic sample. In light of this, the total energy convergence to a negative value in atomic samples indicates thermodynamic equilibrium in samples defined at the IT. The equilibration of the atomic structure was made possible by the simulation's lengthy enough runtime, as seen by this convergence.

a)

b)
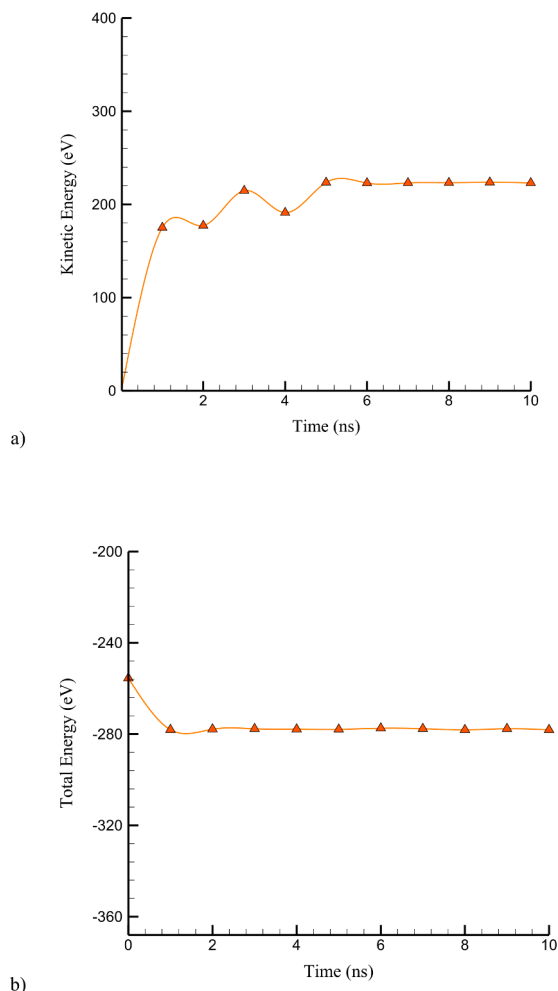
Fig. A-1. The change in a) Kinetic and b) Total energy of the simulated structure.

The study of the thermal behavior of the structure following the combustion process. The parameters of HF, TC, and CE were investigated for this purpose. In addition, maximal density, velocity, and temperature parameters were investigated in order to study atomic behavior.

References

[1] A. Galadima, O. Muraza, Advances in catalyst design for the conversion of methane to aromatics: a critical review, Catal. Surv. Asia 23 (2019) 149–170.
[2] X. Yu, L. Zhu, Y. Wang, D. Filev, X. Yao, Internal combustion engine calibration using optimization algorithms, Appl. Energy 305 (2022) 117894.
[3] X. Li, Z. Peng, Y. Pei, T. Ajmal, K.J. Rana, A. Aitouche, R. Mobasheri, Oxy-fuel combustion for carbon capture and storage in internal combustion engines–A review, Int. J. Energy Res. 46 (2) (2022) 505–522.
[4] J. Krzywanski, T. Czakiert, A. Zylka, W. Nowak, M. Sosnowski, K. Grabowska, D. Skrobek, K. Sztekler, A. Kulakowska, W.M. Ashraf, Modelling of SO2 and NOx

emissions from coal and biomass combustion in air-firing, oxyfuel, iG-CLC, and CLOU conditions by fuzzy logic approach, Energies 15 (21) (2022) 8095.

[5] Z. ur Rahman, X. Wang, J. Zhang, Z. Yang, G. Dai, P. Verma, H. Mikulcic, M. Vujanovic, H. Tan, R.L. Axelbaum, Nitrogen evolution, NOX formation and reduction in pressurized oxy coal combustion, Renew. Sustain. Energy Rev. 157 (2022) 112020.

[6] Z. Chen, Y. Qiao, S. Guan, Z. Wang, Y. Zheng, L. Zeng, Z. Li, Effect of inner and outer secondary air ratios on ignition, C and N conversion process of pulverized coal in swirl burner under sub-stoichiometric ratio, Energy 239 (2022) 122423.

[7] A. Fayyazbakhsh, M.L. Bell, X. Zhu, X. Mei, M. Koutný, N. Hajinajaf, Y. Zhang, Engine emissions with air pollutants and greenhouse gases and their control technologies, J. Clean. Prod. (2022) 134260.

[8] C.E. Baukal Jr, Oxygen-enhanced Combustion, CRC press, 2010.

[9] S.M. Mousavi, F. Sotoudeh, D. Jun, B.J. Lee, J.A. Esfahani, N. Karimi, On the effects of NH3 addition to a reacting mixture of H2/CH4 under MILD combustion regime: numerical modeling with a modified EDC combustion model, Fuel 326 (2022) 125096.

[10] G.B. Ariemma, G. Sorrentino, R. Ragucci, M. de Joannon, P. Sabia, Ammonia/Methane combustion: stability and NOx emissions, Combust. Flame 241 (2022) 112071.

[11] J. Choi, T. Yi, H. Kim, Combustion of a dilute carbon black/ethanol nanofuel droplet in elevated pressure conditions, Fuel 292 (2021) 120376.

[12] S. Nam, H. Kim, Combustion characteristics of a 1-butanol gel fuel droplet in elevated pressure conditions, Fuel 332 (2023) 126173.

[13] H. Liu, J. Liu, J. Yuan, X. Chen, Y. Zhao, W. Xie, Initial temperature effects on the combustion characteristics of Al, Propellants, Explos. Pyrotech. 47 (9) (2022) e202100365.

[14] K. Chen, W. Li, G. Guo, C. Zhu, W. Wu, L. Yuan, Nickel hydroxide nanosheets prepared by a direct manual grinding strategy for high-efficiency catalytic combustion of methane, ACS Omega 7 (10) (2022) 8536–8546.

[15] X. Shao, J. He, Q. Su, D. Zhao, S. Feng, Synergy effect of CuO on CuCo 2 O 4 for methane catalytic combustion, RSC advances 12 (27) (2022) 17490–17497.

[16] J. Banks, "Introduction to Simulation." pp. 7-13..

[17] Z. Liu, K. Zhu, A.M. Abed, D. Toghraie, Effect of a palladium catalyst and initial pressure on methane-air catalytic combustion process in a helical coil microchannel: a molecular dynamics approach, Mol. Catal. 535 (2023) 112868.

[18] M. Feng, X.Z. Jiang, K.H. Luo, A reactive molecular dynamics simulation study of methane oxidation assisted by platinum/graphene-based catalysts, Proc. Combust. Inst. 37 (4) (2019) 5473–5480.

[19] J. Wang, X.Z. Jiang, K.H. Luo, Exploring reaction mechanism for ammonia/methane combustion via reactive molecular dynamics simulations, Fuel 331 (2023) 125806.

[20] X. Liu, M. Zhao, M. Feng, Y. Zhu, Study on mechanisms of methane/hydrogen blended combustion using reactive molecular dynamics simulation, Int. J. Hydrogen Energy 48 (4) (2023) 1625–1635.

[21] N. Habibollahi, A. Abdollahi, S.M. Sajadi, D. Toghraie, S. Emami, M. Shahgholi, M. Inc, Molecular dynamics simulation of combustion behavior of coated aluminum hydride nanoparticles in the oxygenated medium: effects of adding the ethanol atomic coating, Eng. Anal. Bound. Elem. 150 (2023) 180–186.

[22] J. Zeng, L. Cao, M. Xu, T. Zhu, J.Z. Zhang, Complex reaction processes in combustion unraveled by neural network-based molecular dynamics simulation, Nat. Commun. 11 (1) (2020) 5713.

[23] Y. Qiu, W. Zhong, Y. Shao, A. Yu, Reactive force field molecular dynamics (ReaxFF MD) simulation of coal oxy-fuel combustion, Powder Technol. 361 (2020) 337–348.

[24] S. Bhoi, T. Banerjee, K. Mohanty, Insights on the combustion and pyrolysis behavior of three different ranks of coals using reactive molecular dynamics simulation, RSC advances 6 (4) (2016) 2559–2570.

[25] S. Nosé, A unified formulation of the constant temperature molecular dynamics methods, J. Chem. Phys. 81 (1) (1984) 511–519.

[26] W.G. Hoover, Canonical dynamics: equilibrium phase-space distributions, Phys. Rev. 31 (3) (1985) 1695.

[27] M. Foroutan, and S. M. Fatemi, "Molecular Dynamics Simulations of Systems Containing Nanostructures.".

[28] D.H. Brookes, T. Head-Gordon, Family of oxygen–oxygen radial distribution functions for water, J. Phys. Chem. Lett. 6 (15) (2015) 2938–2943.

[29] P. Cicu, P. Demontis, S. Spanu, G.B. Suffritti, A. Tilocca, Electric-field-dependent empirical potentials for molecules and crystals: a first application to flexible water molecule adsorbed in zeolites, J. Chem. Phys. 112 (19) (2000) 8267–8278.

[30] P. Zhang, I.G. Zsély, M. Papp, T. Nagy, T. Turányi, Comparison of methane combustion mechanisms using laminar burning velocity measurements, Combust. Flame 238 (2022) 111867.

[31] L. He, Y. Fan, J. Bellettre, J. Yue, L. Luo, A review on catalytic methane combustion at low temperatures: catalysts, mechanisms, reaction conditions and reactor designs, Renew. Sustain. Energy Rev. 119 (2020) 109589.

[32] X.J. Gu, M.Z. Haq, M. Lawes, R. Woolley, Laminar burning velocity and Markstein lengths of methane–air mixtures, Combust. Flame 121 (1–2) (2000) 41–58.

[33] Y. Yan, W. Pan, L. Zhang, W. Tang, Z. Yang, Q. Tang, J. Lin, Numerical study on combustion characteristics of hydrogen addition into methane–air mixture, Int. J. Hydrogen Energy 38 (30) (2013) 13463–13470.

[34] Y.B. Yang, C. Ryu, A. Khor, N.E. Yates, V.N. Sharifi, J. Swithenbank, Effect of fuel properties on biomass combustion. Part II. Modelling approach—identification of the controlling factors, Fuel 84 (16) (2005) 2116–2130.

[35] J. Liu, X. Guo, ReaxFF molecular dynamics simulation of pyrolysis and combustion of pyridine, Fuel Process. Technol. 161 (2017) 107–115.

[36] N. Pizzolato, C. Fazio, R.M.S. Mineo, D.P. Adorno, Open-inquiry driven overcoming of epistemological difficulties in engineering undergraduates: a case study in the context of thermal science, Phys. Rev. ST Phys. Educ. Res. 10 (1) (2014) 010107.

[37] X. Liu, M. Adibi, M. Shahgholi, I. Tlili, S.M. Sajadi, A. Abdollahi, Z. Li, A. Karimipour, Phase Change Process in a Porous Carbon-Paraffin Matrix with Different Volume Fractions of Copper Oxide Nanoparticles: A Molecular Dynamics Study, Journal of Molecular Liquids, 2022 120296.

[38] H. Geng, Z. Yang, L. Zhang, J. Ran, Y. Chen, Experimental and kinetic study of methane combustion with water over copper catalyst at low-temperature, Energy Convers. Manag. 103 (2015) 244–250.

[39] R.K. Maurya, R.K. Maurya, Luby, Characteristics and Control of Low Temperature Combustion Engines, Springer, 2018.

[40] D.A. Vallero, Air Pollution Calculations: Quantifying Pollutant Formation, Transport, Transformation, Fate and Risks, Elsevier, 2019.

[41] B.G. Miller, Clean Coal Technologies for Advanced Power Generation, Clean Coal Engineering Technology, 2011, pp. 251–300.

[42] M. Zarringhalam, H. Ahmadi-Danesh-Ashtiani, D. Toghraie, R. Fazaeli, Molecular dynamic simulation to study the effects of roughness elements with cone geometry on the boiling flow inside a microchannel, Int. J. Heat Mass Tran. 141 (2019) 1–8, https://doi.org/10.1016/j.ijheatmasstransfer.2019.06.064.

[43] S.-R. Yan, N. Shirani, M. Zarringhalam, D. Toghraie, Q. Nguyen, A. Karimipour, Prediction of boiling flow characteristics in rough and smooth microchannels using molecular dynamics simulation: investigation the effects of boundary wall temperatures, J. Mol. Liq. 306 (112937) (2020) 112937, https://doi.org/10.1016/j.molliq.2020.112937.